A tunable multi-band metamaterial design using micro-split SRR structures

Evren Ekmekci[1, 2,*], Kagan Topalli[1], Tayfun Akin[1], and Gonul Turhan-Sayan[1]

[1] *Dept. Electrical and Electronics Eng., Middle East Technical University, Ankara, TURKEY.*
[2] *Dept. Electronics and Communication Eng., Suleyman Demirel University, Isparta, TURKEY.*
** eekmekci@metu.edu.tr*

Abstract: This paper presents the results of a feasibility study for the design of multi-band tunable metamaterials based on the use of micro-split SRR (MSSRR) structures. In this study, we have designed and constructed a conventional split-ring resonator (SRR) unit cell (type A) and two modified SRR unit cells having the same design parameters except that they contain two (type B) or four (type C) additional micro-splits on the outer square ring, along the arm having the main split. Transmission characteristics of the resulting MSSRR cells are obtained both numerically and experimentally and compared to those of the ordinary SRR unit cell. It is observed that the presence of the additional micro-splits leads to the increase of resonance frequency by substantial amounts due to the series capacitance effect. Next, we have designed and constructed 2×2 homogeneous arrays of magnetic resonators which consist of the same type of cells (either A, or B, or C). Such MSSRR blocks are found to provide only a single frequency band of operation around the magnetic resonance frequency of the related unit cell structure. Finally, we have designed and constructed 2×2 and 3×2 inhomogeneous arrays which contain columns of different types of metamaterial unit cells. We have shown that these inhomogeneous arrays provide two or three different frequency bands of operations due to the use of different magnetic resonators together. The number of additional micro-splits in a given MSSRR cell can be interactively controlled by various switching technologies to modify the overall metamaterial topology for the purpose of activating different sets of multiple resonance frequencies. In this context, use of electrostatically actuated RF MEMS switches is discussed, and their implementation is suggested as a future work, to control the states of micro-splits in large MSSRR arrays to realize tunable multi-band metamaterials.

OCIS codes: (160.3918) Metamaterials; (350.4010) Microwaves; (260.5740) Resonators.

References and Links

1. V. G. Veselago, "The electrodynamics of substances with simultaneously negative values of ε and μ," Sov. Phys. Usp. **10**(4), 509–514 (1968).
2. J. B. Pendry, A. J. Holden, D. J. Robbins, and W. J. Stewart, "Low frequency plasmons in thin-wire structures," J. Phys. Condens. Matter **10**(22), 4785–4809 (1998).
3. J. B. Pendry, A. J. Holden, D. J. Robbins, and W. J. Stewart, "Magnetism from conductors and enhanced nonlinear phenomena," IEEE Trans. Microw. Theory Tech. **47**(11), 2075–2084 (1999).
4. J. D. Baena, R. Marques, F. Medina, and J. Martel, "Artificial magnetic metamaterial design by using spiral resonators," Phys. Rev. B **69**(1), 014402 (2004).
5. E. Ekmekci, and G. Turhan-Sayan, "Investigation of Permittivity and Permeability for a Novel V-Shaped Metamaterial Using Simulated S-Parameters," in *Proceedings of 5th International Conference on Electrical and Electronics Engineering*, (The Chamber of Turkish Electrical Engineers, Bursa, Turkey, 2007), pp. 251–254.
6. I. Bulu, H. Caglayan, and E. Ozbay, "Experimental demonstration of labyrinth-based left-handed metamaterials," Opt. Express **13**(25), 10238–10247 (2005).
7. E. Özbay, I. Bulu, and H. Caglayan, "Transmission, reflection and focusing properties of labyrinth based left-handed metamaterials," Phys. Status Solidi **244**(4), 1202–1210 (2007).

#113866 - $15.00 USD Received 6 Jul 2009; revised 16 Aug 2009; accepted 19 Aug 2009; published 26 Aug 2009

8. K. Aydin, I. Bulu, K. Guven, M. Kafesaki, C. M. Soukoulis, and E. Ozbay, "Investigation of magnetic resonances for different split-ring resonator parameters and designs," N. J. Phys. **7**(168), 1–15 (2005).
9. Z. Sheng, and V. V. Varadan, "Tuning the effective properties of metamaterials by changing the substrate properties," J. Appl. Phys. **101**(1), 014909 (2007).
10. E. Ekmekci, and G. Turhan-Sayan, "Comparative investigation of resonance characteristics and electrical size of the double-sided SRR, BC-SRR and conventional SRR type metamaterials for varying substrate parameters," Prog. Electromagn. Res. B **12**, 35–62 (2009).
11. Q. Zhao, L. Kang, B. Du, B. Li, J. Zhou, H. Tang, X. Liang, and B. Zhang, "Electrically tunable negative permeability metamaterials based on nematic liquid crystals," Appl. Phys. Lett. **90**(1), 011112 (2007).
12. F. Zhang, L. Kang, Q. Zhao, J. Zhou, X. Zhao, and D. Lippens, "Magnetically tunable left handed metamaterials by liquid crystal orientation," Opt. Express **17**(6), 4360–4366 (2009).
13. S. Xiao, U. K. Chettiar, A. V. Kildishev, V. Drachev, I. C. Khoo, and V. M. Shalaev, "Tunable magnetic response of metamaterials," Appl. Phys. Lett. **95**(3), 033115 (2009).
14. O. Reynet, and O. Acher, "Voltage controlled metamaterial," Appl. Phys. Lett. **84**(7), 1198–1200 (2004).
15. I. Gil, J. Bonache, J. García- García, and F. Martín, "Tunable metamaterial transmission lines based on varactor-loaded split-ring resonators," IEEE Trans. Microw. Theory Tech. **54**(6), 2665–2674 (2006).
16. H. Chen, B. Wu, L. Ran, T. M. Grzegorczyk, and J. A. Kong, "Controllable left-handed metamaterial and its application to streerable antenna," Appl. Phys. Lett. **89**(5), 053509 (2006).
17. K. Aydin, and E. Ozbay, "Capacitor-loaded split ring resonators as tunable metamaterial components," J. Appl. Phys. **101**(2), 024911 (2007).
18. D. Wang, L. Ran, H. Chen, M. Mu, J. A. Kong, and B.-I. Wu, "Active left-handed material collaborated with microwave varactors," Appl. Phys. Lett. **91**(16), 164101 (2007).
19. A. Vélez, J. Bonache, and F. Martín, "Varactor-loaded complementary split ring resonators (VLCSRR) and their application to tunable metamaterial transmission lines," IEEE Microw. Wirel. Compon. Letters **18**(1), 2008.
20. L. Kang, Q. Zhao, H. Zhao, and J. Zhou, "Ferrite-based magnetically tunable left-handed metamaterial composed of SRRs and wires," Opt. Express **16**(22), 17269–17275 (2008).
21. L. Kang, Q. Zhao, H. Zhao, and J. Zhou, "Magnetically tunable negative permeability metamaterial composed by split ring resonators and ferrite rods," Opt. Express **16**(12), 8825–8834 (2008).
22. T. H. Hand, and S. A. Cummer, "Frequency tunable electromagnetic metamaterial using ferroelectric loaded split rings," J. Appl. Phys. **103**(6), 066105 (2008).
23. M. Gil, C. Damm, A. Giere, M. Sazegar, J. Bonache, R. Jakoby, and F. Martín, "Electrically tunable split-ring resonators at microwave frequencies based on barium-strontium-titanate thick films," Electron. Lett. **45**(8), 417 (2009).
24. H. T. Chen, J. F. O'Hara, A. K. Azad, A. J. Taylor, R. D. Averitt, D. Shrekenhamer, and W. J. Padilla, "Experimental demonstration of frequency agile terahertz metamaterials," Nat. Photonics **2**(5), 295–298 (2008).
25. K. A. Boulais, D. W. Rule, S. Simmons, F. Santiago, V. Gehman, K. Long, and A. Rayms-Keller, "Tunable split-ring resonator for metamaterials using photocapacitance of semi-insulting GaAs," Appl. Phys. Lett. **93**(4), 043518 (2008).
26. J. Han, A. Lakhtakia, and C.-W. Qiu, "Terahertz metamaterials with semiconductor split-ring resonators for magnetostatic tunability," Opt. Express **16**(19), 14390–14396 (2008).
27. J. Han, and A. Lakhtakia, "Semiconductor split,ring resonators for thermally tunable terahertz metamaterials," J. Mod. Opt. **56**(4), 554–557 (2009).
28. I. Gil, F. Martín, X. Rottenberg, and W. De Raedt, "Tunable stop-band filter at Q-band based on RF-MEMS metamaterials," Electron. Lett. **43**(21), 1153 (2007).
29. T. Hand, and S. Cummer, "Characterization of tunable metamaterial elements using MEMS switches," IEEE Antennas Wirel. Propag. Lett. **6**(11), 401–404 (2007).
30. S. O'Brien, D. McPeake, S. A. Ramakrishna, and J. B. Pendry, "Near-infrared photonic band gaps and nonlinear effects in negative magnetic materials," Phys. Rev. B **69**(24), 241101 (2004).
31. R. S. Penciu, K. Aydin, M. Kafesaki, Th. Koschny, E. Ozbay, E. N. Economou, and C. M. Soukoulis, "Multi-gap individual and coupled split-ring resonator structures," Opt. Express **16**(22), 18131–18144 (2008).
32. D.-H. Kwon, D. H. Werner, A. V. Kildishev, and V. M. Shalaev, "Near-infrared metamaterials with dual-band negative-index characteristics," Opt. Express **15**(4), 1647–1652 (2007).
33. Y. Yuan, C. Bingham, T. Tyler, S. Palit, T. H. Hand, W. J. Padilla, D. R. Smith, N. M. Jokerst, and S. A. Cummer, "Dual-band planar electric metamaterial in the terahertz regime," Opt. Express **16**(13), 9746–9752 (2008).
34. K. Topalli, A. Civi, S. Demir, S. Koc, and T. Akin, "A monolithic phased array using 3-bit DMTL RF MEMS phase shifters," IEEE Trans. Microw. Theory Tech. **56**(2), 270–277 (2008).
35. G. M. Rebeiz, *RF MEMS theory, design, and technology*, (John Wiley & Sons, Hoboken, NJ, 2003).
36. A. B. Kaul, E. W. Wong, L. Epp, and B. D. Hunt, "Electromechanical carbon nanotube switches for high-frequency applications," Nano Lett. **6**(5), 942–947 (2006).
37. F. Bilotti, A. Toscano, and L. Vegni, "Design of spiral and multiple split-ring resonators for the realization of miniaturized metamaterial samples," IEEE Trans. Antenn. Propag. **55**(8), 2258–2267 (2007).
38. K. B. Alici, F. Bilotti, L. Vegni, and E. Ozbay, "Miniaturized negative permeability materials," Appl. Phys. Lett. **91**(7), 071121 (2007).
39. F. Aznar, J. García-García, M. Gil, J. Bonache, and F. Martín, "Strategies for the miniaturization of metamaterial resonators," Microw. Opt. Technol. Lett. **50**(5), 1263–1270 (2008).
40. E. Ekmekci, and G. Turhan-Sayan, "Reducing the electrical size of magnetic metamaterial resonators by geometrical modifications: a comparative study for single-sided and double-sided multiple SRR, spiral and U-

#113866 - $15.00 USD Received 6 Jul 2009; revised 16 Aug 2009; accepted 19 Aug 2009; published 26 Aug 2009

Spiral resonators," in *Proceedings of IEEE International Symposium on Antennas & Propagation*, (IEEE Antennas and Propagation Society, San Diego, 2009), pp. 1484–1487.
41. D. K. Ghodgaonkar, V. V. Varadan, and V. K. Varadan, "Free-space measurement of complex permittivity and complex permeability of magnetic materials at microwave frequencies," IEEE Trans. Instrum. Meas. **39**(2), 387–394 (1990).

1. Introduction

Negative index metamaterials (NIM) are engineered materials that show simultaneously negative values of effective permittivity (ε_{eff}) and effective permeability (μ_{eff}) values over a common frequency band [1]. Such materials have interesting and useful properties such as backward propagation, reverse Doppler effect and reverse Vavilov-Cerenkov effect which are not possessed by natural materials [1]. Fortunately, fabrication of metamaterials can be easily accomplished by using the well-known lithographic techniques. It is possible to obtain negative values of ε_{eff} over quite wide frequency bands using periodic thin wire arrays [2]. Negative values of μ_{eff} can be obtained, on the other hand, by using special magnetic resonator structures such as SRRs, spiral resonators (SR), V-shaped resonators, and labyrinth resonators [3–7]. The frequency bandwidth of such magnetic resonator arrays (with negative μ_{eff} property) is usually a small fraction of the bandwidth of the periodic thin wire arrays (with negative ε_{eff} property). Therefore, tuning the left-handed operation bandwidth of a composite material, which is composed of both thin wire array and magnetic resonator array, essentially requires tuning the resonance frequency of the magnetic resonator structure.

In literature, there are various approaches reported for tuning the resonance frequency of magnetic resonators. A common approach to select the resonance frequency of a magnetic resonator is to change the geometrical parameters of the metallic inclusions (i.e. strip width, separation between the rings, split widths, gap widths, unit cell dimension, etc.) [8] or to play with the thickness and dielectric constant of the substrate [9,10]. Obviously, it is not possible to change geometrical parameters of the already printed metallic inclusions or the parameters of the substrate unless some sophisticated techniques are used for real-time tuning. Use of liquid crystals [11–13], lumped capacitors or varactors [14–19], ferromagnetic [20,21] and ferroelectric [22,23] techniques, semiconductors [24–27], and microelectromechanical (MEMS) switches [28,29] have been suggested in literature for tuning metamaterial devices in various applications.

In this study, we suggest an alternative split-ring resonator topology that provides not only multi-band operation at two or more resonance frequencies but also lends itself to adaptive tuning. As the first step of this approach, a uniform array of identical micro-split SRR (MSSRR) cells is designed and fabricated such that each MSSRR cell has N pairs of very narrow (in the order of tens of micrometers for X-band designs) additional splits etched on both sides of the main split along the external ring. A maximum possible resonance frequency f_N is realized with this homogeneous array because the equivalent capacitance of each unit cell is minimized due to the series capacitances introduced by each micro-split. Since the gap width of the additional micro-splits (g_{ms}) is designed to be much smaller than the width of the main split (g), their (on/off) states can be conveniently changed by electrostatically actuated RF MEMS switches [28,29] that should be implemented during the fabrication of the MSSRR array. If all of the micro-splits in the array are closed by setting the MEMS switches to their "ON" state, a homogeneous array of traditional SRRs (having their main gaps only) is obtained providing the minimum available resonance frequency f_1. In principle, any combination out of N possible resonance frequencies f_1, f_2,…, f_N can be realized by controlling the switching states associated with the micro-splits in properly chosen columns of the MSSRR array. The maximum value of N is basically limited by the condition that the dimensions of the composite unit cell (formed as a collection of N individual MSSRR cells) must be a small fraction of the wavelength even at the highest resonance frequency. As to be demonstrated in the rest of this paper, in the case of N=3 for instance, the single and multi-band operations having the sets of resonance frequencies $\{f_1\}$, $\{f_2\}$, $\{f_3\}$, $\{f_1\ f_2\}$,$\{f_1\ f_3\}$,$\{f_2\ f_3\}$ and $\{f_1\ f_2\ f_3\}$ can be provided by a single MSSRR array topology. In addition to demonstrating the possibility of actual multi-band operation in inhomogeneous MSSRR

#113866 - $15.00 USD Received 6 Jul 2009; revised 16 Aug 2009; accepted 19 Aug 2009; published 26 Aug 2009

arrays, another contribution of this work is to suggest a feasible approach for adaptive tuning of the MSSRR arrays based on the well established MEMS technology. As the actual implementation of RF MEMS switches in large MSSRR arrays has not been accomplished yet, we have followed a proof-of-concept approach and placed copper strips across the micro-splits to simulate the "ON" states of the ideal switches both in our numerical simulations and experiments. Design, fabrication and testing of MSSRR arrays integrated with electrostatically actuated RF MEMS switches [34] are planned as a future work to demonstrate the actual adaptive tuning of multi-band operation.

At this point, we need to emphasize a few important issues to clarify the intended contributions of this paper: First of all, controlling the resonance frequency of an SRR by using additional distributed gaps is a well known approach studied in various papers [6–8,30,31]. In most of those studies, however, multiple gaps of equal widths have been employed leading to very large increases in resonance frequency. For example, resonance frequencies of the single-gap, double-gap and four-gap SRR (single ring) cells are reported to be about 4.5 GHz, 8 GHz and 13 GHz, respectively in [8]. On the other hand, use of conventional SRR cells (without any additional small splits) with varying main gap widths was not a proper solution either for two reasons; varying the width of main gap produces quite small changes in resonance frequency (for example, an increase from 3.6 GHz to 3.8 GHz is reported in [8] for a change of gap width from 0.2 mm to 0.5 mm), and closing the one and only gap of an SRR cell by a switching mechanism (for the purpose of adaptive tuning) completely annihilates the associated resonance. Controlling the state of the main gap by a single RF MEMS switch operating as a varactor could be another alternative but this approach is not considered to be useful either as this method is known to provide only a small range of frequency tuning [35]. Therefore, to obtain intermediate size shifts (about one GHz in X-band, for instance) in resonance frequency, we found that the combination of a main gap and a number of narrower gaps in the outer ring of an SRR cell is definitely more useful. Also, adaptive control of the states of such narrower micro-gaps is known to be easier with technologies like MEMS switching.

Secondly, metamaterial design studies with dual-band operation are already reported [32,33] in THz and near-infrared regions. Each of these recent studies successfully demonstrates the realization of two distinct operational bandwidths using an array of composite-cells which are composed of two individual resonators of different physical dimensions and hence they have different resonance frequencies. However, the dual-band metamaterial topologies reported in these references are not suitable for adaptive frequency tuning as their resonance frequencies are fixed permanently during the fabrication process. In the present paper, on the other hand, the composite unit cells are composed of two or more micro-split SRR cells whose resonance frequencies can be externally adjusted after the fabrication of the metamaterial array by means of suitable switching techniques.

Finally, the suggested MSSRR-based multi-band metamaterial design approach is expected to be still useful in millimeter wave, THz and near-infrared regions with proper scaling of the unit cell dimensions. As the wavelength gets smaller, the geometrical shapes of these sub-wavelength structures should be made simpler for easier fabrication. Single ring SRR unit cells with additional nano-splits may be suitable at higher frequencies. Nano-switching techniques [36] would possibly be needed to control the switching states of nano-splits if adaptive tunability is required.

2. Design

The schematic views of the unit cell structures proposed in this study are given in Fig. 1. A conventional SRR structure (unit cell A), an SRR with two additional micro-splits (unit cell B) and an SRR with four additional micro-splits (unit cell C) are shown in parts (a), (b) and (c) of Fig. 1, respectively. All these square shaped unit cells have the same side length of l=2.8 mm, main split width of g=0.3 mm, metal strip width of w=0.3 mm and inner/outer strip separation length of s=0.3 mm. For the unit cell B, the additional design parameters shown in Fig. 1(b) are chosen to be l_1=0.85 mm, l_2=0.35 mm and l_3=1.25 mm. Similarly for the unit cell

#113866 - $15.00 USD Received 6 Jul 2009; revised 16 Aug 2009; accepted 19 Aug 2009; published 26 Aug 2009

C, the additional design parameters are chosen as l_1=0.45 mm, l_2=0.35 mm, l_3=0.35 mm and l_4=1.25 mm. Thus, the width of each additional micro-split gap (g_{ms}) is set to be 50 microns. The A type, B type and C type MSSRR magnetic resonator unit cells and their arrays are fabricated at Middle East Technical University (METU) MEMS Center Fabrication Facilities with 100 Å/0.5 μm Ti/Au patterned lithography on a 4" glass substrate having a thickness of 500 μm, relative permittivity of 4.6 and loss tangent of 0.01. The unit cell structures are diced from glass substrate to obtain a total unit cell dimension of 4 mm × 4 mm including the blank glass areas outside the borders of the SRRs. Prior to fabrication, the transmission and reflection spectra of all those three different unit cells and their arrays are numerically simulated using the Ansoft's HFSS software, which is a full wave solver based on the finite elements method. The same set of geometrical parameters and material parameters are used both in numerical simulations and in fabrication of the sample structures. Furthermore, the experimental setup (described in section 3) used in measurements is identically simulated in HFSS simulations for meaningful comparison of numerical and experimental results.

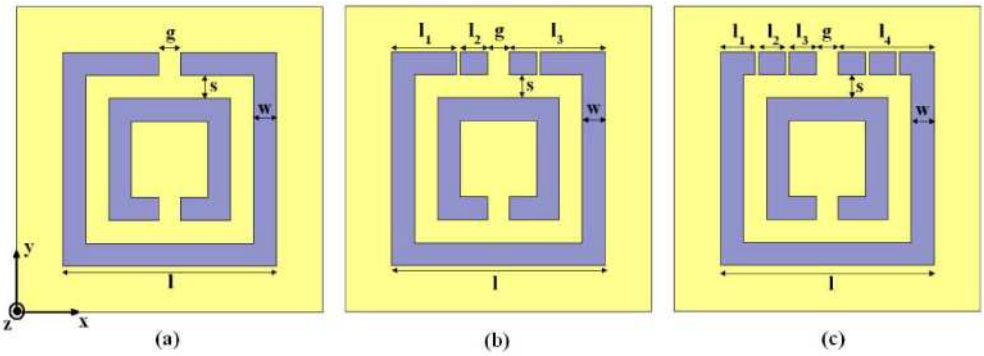

Fig. 1. Schematic views of (a) Unit cell A, (b) unit cell B, and (c) unit cell C.

3. Simulations and experiments

In this study, the structure under investigation is placed in an X-band waveguide with dimensions of 22.86 mm × 10.16 mm × 12.8 mm as shown in Fig. 2. The schematic demonstration of the experimental setup is given in Fig. 2(a) while a picture of the actual experimental setup is shown in Fig. 2(b),. This experimental setup is identically simulated in HFSS modeling as indicated before. Therefore, planar faces of the computational volume, which are perpendicular to both y and z axes, are modeled to be perfect electric conductor (PEC) boundaries as they coincide with the metallic walls of the waveguide. The faces perpendicular to the x axis are modeled to be the input/output ports. The resonator structures are excited by an electromagnetic wave with propagation vector (***k***) along the x-axis, electric filed vector (***E***) along the y-axis and magnetic field vector (***H***) along the z-axis. The experimental results are measured over the frequency range from 8 GHz to 12 GHz by Agilent's 8720D network analyzer using TRL calibration.

#113866 - $15.00 USD Received 6 Jul 2009; revised 16 Aug 2009; accepted 19 Aug 2009; published 26 Aug 2009

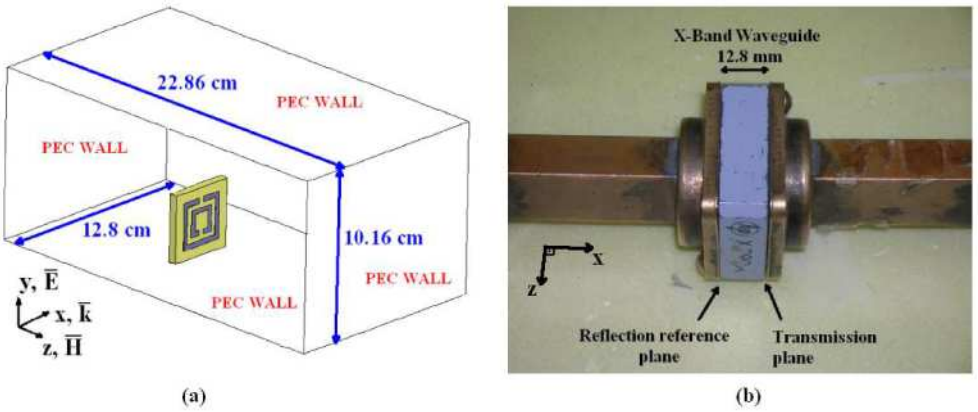

Fig. 2. (a) Schematic of simulation and experimental setup, (b) picture of experimental setup.

4. Results

In the present section, we report detailed experimental and numerical results for some SRR and MSSRR unit cells/arrays to demonstrate the multi-band operation property of inhomogeneous MSSRR arrays and the feasibility for their adaptive tuning. For this purpose, we mainly observe the transmission characteristics (i.e. magnitude of S_{21} scattering parameter spectra) for both unit cells and homogeneous/inhomogeneous small-sized MSSRR arrays.

4.1 SRR and MSSRR unit cells

In this sub-section, we investigate the transmission characteristics of SRR and MSSRR unit cells. Transmission characteristics as well as the photographs of the fabricated unit cells A, B and C are given in Fig. 3, 4 and 5, respectively. Experimental results show that while the unit cell A resonates at 9.48 GHz, the unit cells B and C resonate at 10.58 and 11.41 GHz, respectively. These results demonstrate that there is an appreciable shift in the resonance frequency (about 11.6% for the unit cell B and about 20.4% for the unit cell C with respect to the unit cell A) due to the series capacitance effects caused by additional micro-splits [31]. Herein, the simulation results show good agreement with the measurements.

4.2 Small-sized homogeneous arrays of SRRs or MSSRRs

In this sub-section we investigate the transmission characteristics of small-sized homogeneous SRR or MSSRR arrays. Transmission characteristics and the photographs of 2×2 homogeneous arrays, which consist of only one type of unit cells (either A, or B, or C) are given in Fig. 6, 7 and 8, respectively. It is important to emphasize that each array structure is found to resonate in the vicinity of the resonance frequency of the corresponding unit cell. However, unlike the unit cells, these homogeneous arrays display two resonance frequencies close to each other. This behavior can be explained by the strong coupling effects between neighboring unit cells along the propagation direction as also discussed in [31]. Moreover, a wider stop bandwidth and a lower transmission minimum occur in the transmission characteristics of these array structures.

#113866 - $15.00 USD Received 6 Jul 2009; revised 16 Aug 2009; accepted 19 Aug 2009; published 26 Aug 2009

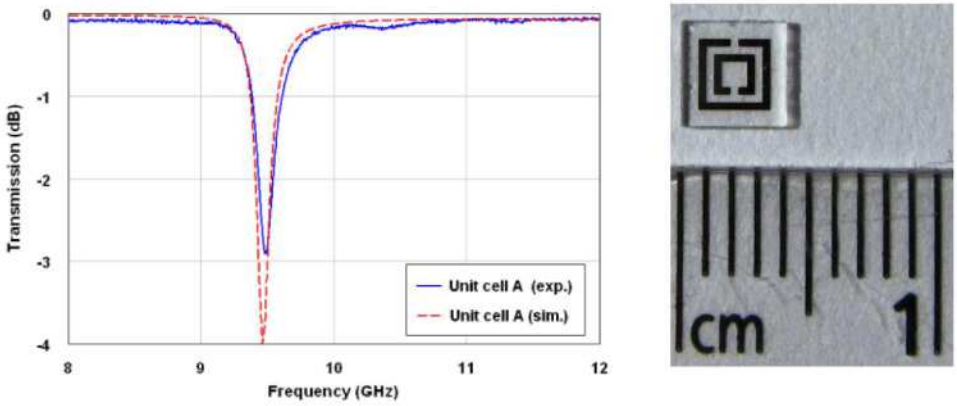

(a) (b)

Fig. 3. (a) Transmission characteristics of the type A unit cell. (b) Photograph of the actual resonator.

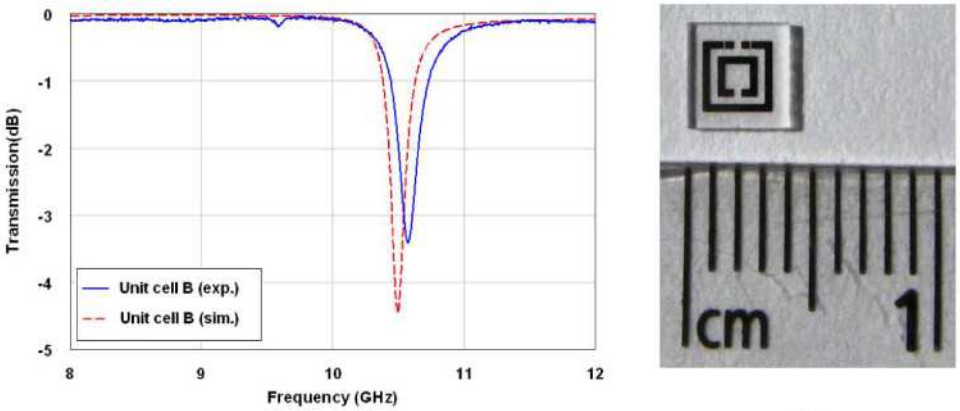

(a) (b)

Fig. 4. (a) Transmission characteristics of the type B unit cell. (b) Photograph of the actual resonator.

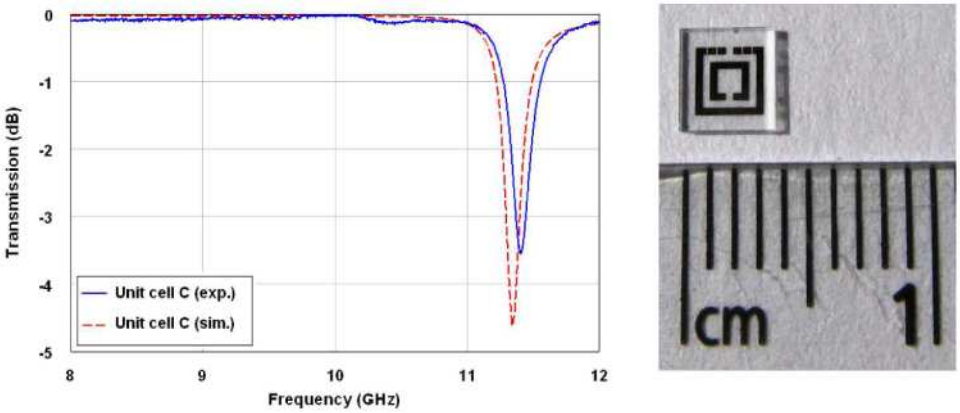

(a) (b)

Fig. 5. (a) Transmission characteristics of the type C unit cell. (b) Photograph of the actual resonator.

#113866 - $15.00 USD Received 6 Jul 2009; revised 16 Aug 2009; accepted 19 Aug 2009; published 26 Aug 2009

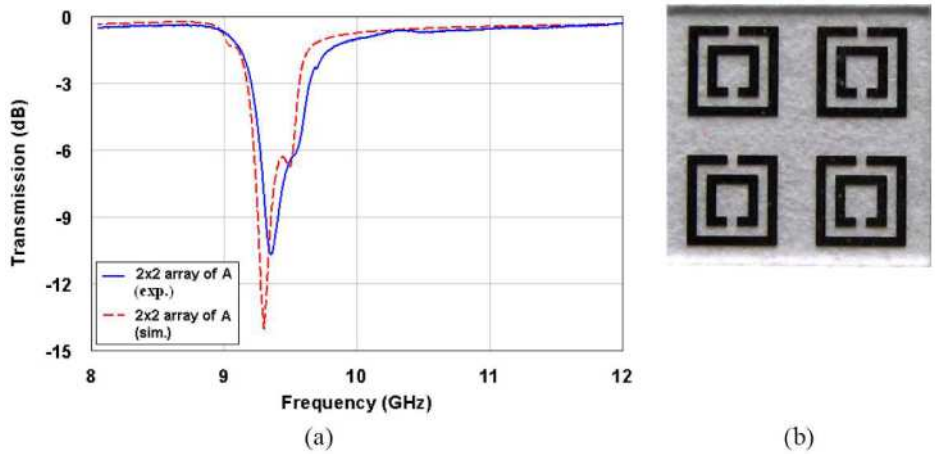

Fig. 6. (a) Transmission characteristics of the 2×2 array of type A unit cell. (b) Photograph of the array.

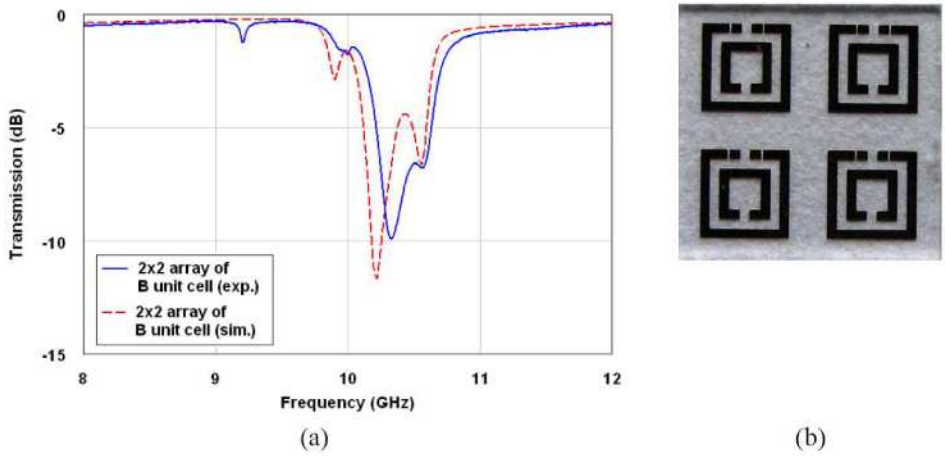

Fig. 7. (a) Transmission characteristics of the 2×2 array of type B unit cell. (b) Photograph of the array.

#113866 - $15.00 USD Received 6 Jul 2009; revised 16 Aug 2009; accepted 19 Aug 2009; published 26 Aug 2009

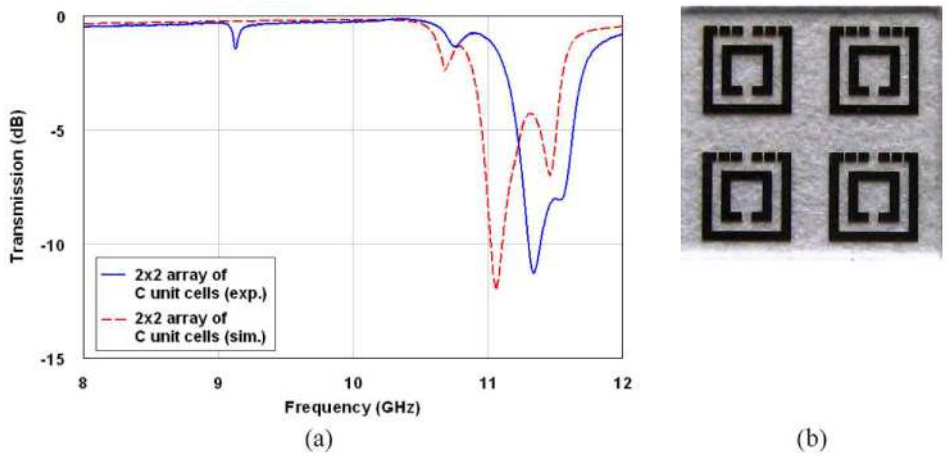

Fig. 8. (a) Transmission characteristics of the 2×2 array of type C unit cell. (b) Photograph of the array.

4.3 Small-sized inhomogeneous arrays of SRRs and MSSRRs

In this sub-section, we investigate the transmission characteristics of three different inhomogeneous arrays of SRRs and MSSRRs, which display dual-band and triple-band operations. The first array consists of two unit cells of type B in the first column and two unit cells of type A in the second column. The simulated and measured transmission characteristics for this array are given in Fig. 9 (a) showing two distinct resonance frequencies; the lower one belongs to the pair of type A resonators and the higher one belongs to the type B resonators. The photograph of this array is also given in Fig. 9(b). Similarly, the second inhomogeneous array shown in Fig. 10 consists of two unit cells of type C in the first column and two unit cells of type A in the second column. Again, the simulated and measured transmission characteristics given in Fig. 10 (a) show two distinct resonance frequencies, one belongs to the pair of type A resonators and the other belongs to pair of type C resonators.

Lastly, we design and fabricate a 3×2 inhomogeneous array which consists of type A (in column 1), type B (in column 2) and type C (in column 3) unit cells. Figure 11 shows the transmission characteristics and the photograph of this array. As expected, the transmission spectra shown in Fig. 12 (a) has three different resonant frequencies due to three different types of unit cells.

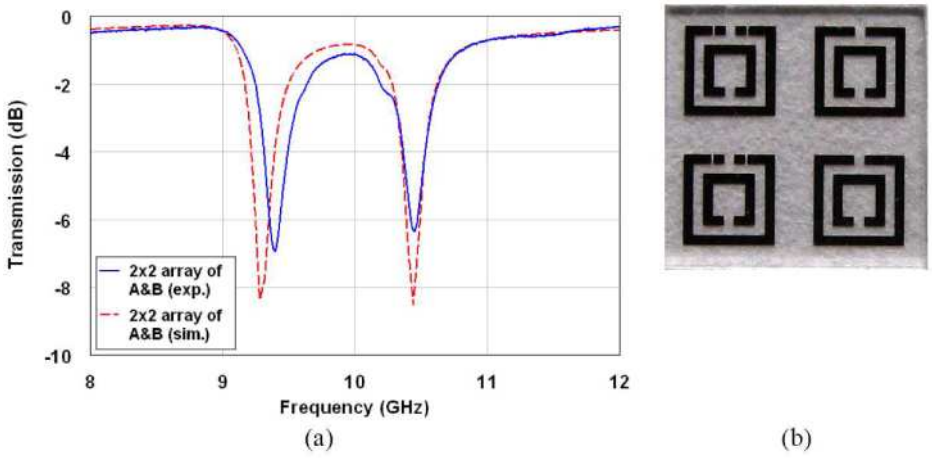

Fig. 9. (a) Transmission characteristics of the 2×2 inhomogeneous array of type A (in column 2) and type B (in column 1) resonators. (b) Photograph of the array.

#113866 - $15.00 USD Received 6 Jul 2009; revised 16 Aug 2009; accepted 19 Aug 2009; published 26 Aug 2009

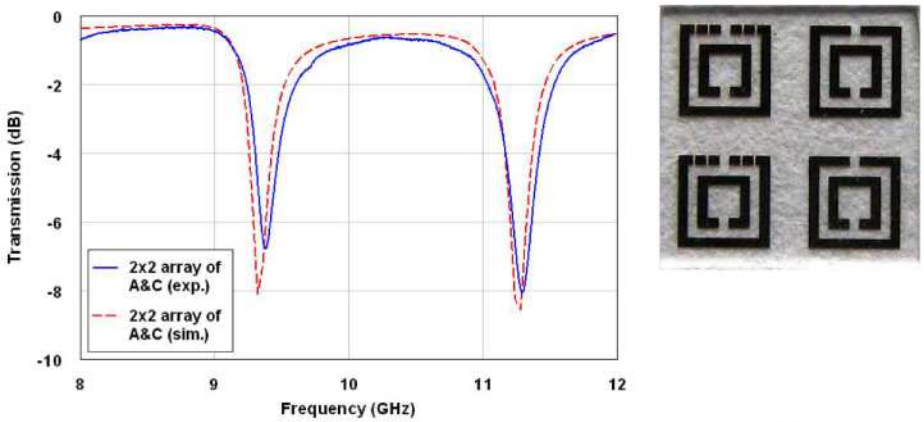

Fig. 10. (a) Transmission characteristics of the 2×2 inhomogeneous array of type A (in column 2) and type C (in column 1) resonators. (b) Photograph of the array.

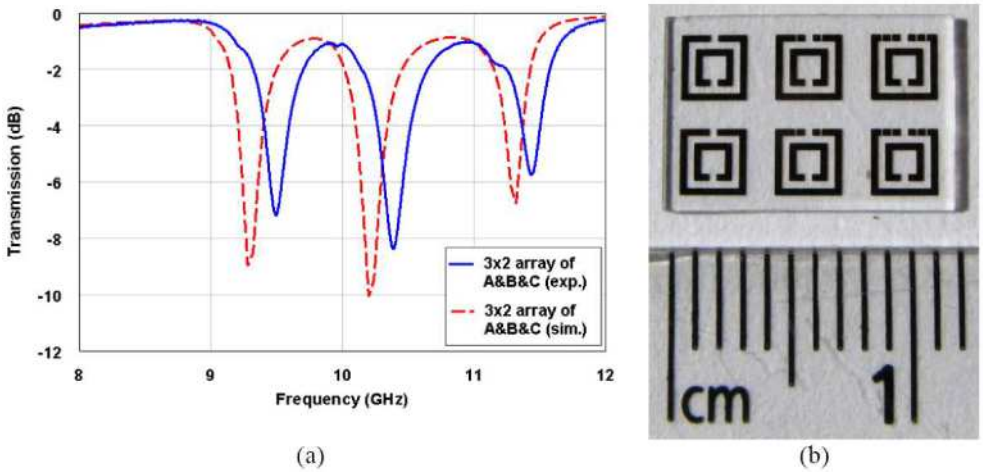

Fig. 11. (a) Transmission characteristics of the 3×2 inhomogeneous array of type A (in column1), type B (in column 2) and type C (in column 3) resonators. (b) Photograph of the array.

4.4. Switching for adaptive tuning of multi-band operation

So far in this study, we have demonstrated the possibility of double-band and three-band magnetic resonator operations using inhomogeneous micro-split SRR arrays. Adaptive tuning of the resonance frequencies in such multi-band design applications is possible if the switching states of the micro-splits in the selected columns of the MSSRR arrays can be efficiently controlled. For better visualization, Fig. 12 shows the schematic view of the switching representation for the unit cell C. Herein, S1, S2, S3, and S4 are the switches that are placed across the micro-splits of the structure. It is clear that, the unit cell B can be realized for the closed-down states of the switches S1 and S4, and also the unit cell A can be realized for the closed-down states of all four switches S1, S2, S3, and S4. In this paper, ideal closed-down switching states of the micro-splits are simulated by metallization for a simplified proof of concept. However, we intend to realize the suggested adaptively tunable MSSRR design by using electrostatically actuated RF MEMS switches fabricated in the facilities of the METU MEMS Center [34] as a future work.

#113866 - $15.00 USD Received 6 Jul 2009; revised 16 Aug 2009; accepted 19 Aug 2009; published 26 Aug 2009

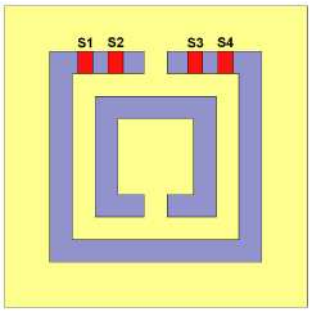

Fig. 12. Schematic view of the switching representation for type C resonator.

5. An alternative three-band metamaterial design with smaller electrical size

The 3×2 inhomogeneous array shown in Fig. 11 provides a successful design for a three-band magnetic resonator. However, the length of the resulting composite cell (composed of A, B and C type SRR cells) along the propagation direction is close to the half wavelength at the highest resonance frequency. Therefore, the interpretation of an array of such composite cells as a homogeneous metamaterial medium is questionable. Certain techniques for better miniaturization could be applied to this composite cell design to shift its resonance frequencies to lower values while keeping the overall composite cell size the same. In literature, there are several useful studies on miniaturized metamaterial structures to provide a better effective medium approach. A simple and useful technique is to increase the dielectric constant of the substrate [9,10]. Increasing the relative permittivity of the substrate increases the total effective capacitance, hence decreases the resonance frequency and the electrical size of the structure. Another approach proposes the use of broad-side coupling for miniaturization purpose [10,39,40]. Lastly, increasing the number of internal rings in multiple SRR and double-sided multiple SRR unit cells becomes quite useful to obtain miniaturized metamaterial structures [37,38,40].

Although the above mentioned techniques are valid and applicable to our composite unit cell structure shown in Fig. 11(b), we can still propose an alternative composite cell arrangement with reduced physical dimensions. Figure 13 shows the schematic representation and dimensions for this new composite unit cell. Herein, type A, type B, and type C structures are positioned along z direction to form a composite cubic cell, with the side length of 4 mm. The magnitude and phase spectra of the complex scattering parameters S_{21} and S_{11} (simulated by HFSS using the previously specified design parameters and the waveguide setup shown in Fig. 2) are plotted in Fig. 14(a) and Fig. 14(b), respectively, for this new composite cell. Locations of the transmission minimums seen in Fig. 14 (a) reveals that this alternative structure provides a three-band operation at the same resonance frequencies as the electrically larger unit cell described earlier. In conclusion, the electrical size of this new three-band composite cell is one third of the electrical size of the former three-band design. The ratio of physical cell size to the wavelength at the highest frequency is close to seven. Hence, retrieval of the effective medium parameters ε_{eff} and μ_{eff} from the complex scattering parameters [41] is meaningful. Real and imaginary parts of the effective permittivity and the effective permeability are plotted in Fig. 15 (a) and Fig. 15(b), respectively. Real part of the effective permittivity stays in positive values while the real part of the effective permeability becomes negative at the resonance frequencies, as expected.

6. Conclusion

In this study, we have proposed the micro-split SRR (MSSRR) type unit cell structures to be used for multi-band and tunable metamaterial design. The on/off state of the extremely narrow additional splits of MSSRRs can be efficiently controlled in microwave frequencies by proper switching techniques such as the RF MEMS switching technique. We have demonstrated that

#113866 - $15.00 USD Received 6 Jul 2009; revised 16 Aug 2009; accepted 19 Aug 2009; published 26 Aug 2009

the resonance frequency of a MSSRR cell can be easily increased by additional micro-splits which effectively reduce the equivalent capacitance of the SRR unit cell. Next, we have investigated the transmission properties of the small-sized homogeneous and inhomogeneous MSSRR arrays to demonstrate the feasibility of multiple frequency band metamaterial designs. For this purpose, dual-band and triple-band resonator structures have been designed, simulated, constructed and experimentally tested over the X-band microwave frequencies with quite satisfactory agreement between simulations and measurements. Also, an electrically smaller triple-band composite MSSRR unit cell is designed and simulated. The effective permittivity and effective permeability parameters are retrieved for this design revealing the presence of magnetic resonances at the resonance frequencies around 9.4 GHz, 10.5 GHz and 11.4 GHz, as expected.

Based on all these investigations, it is concluded that a homogeneous array of MSSRRs can be adaptively turned into different inhomogeneous MSSRR arrays by using proper switching techniques such as RF MEMS switches to change the states of micro-splits in selected columns simultaneously. While we have suggested and thoroughly discussed the feasibility of tunable multi-band magnetic resonator design in this paper, applications involving actual RF MEMS switches are planned as a future work.

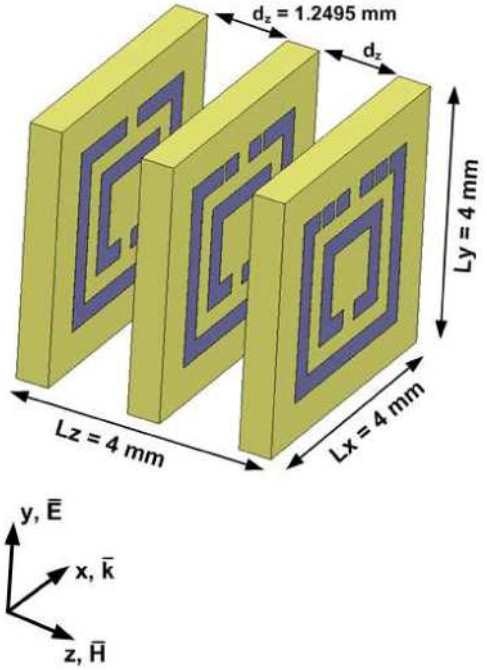

Fig. 13. Schematic representation and dimensions for the alternative electrically small composite unit cell providing a three-band operation.

#113866 - $15.00 USD Received 6 Jul 2009; revised 16 Aug 2009; accepted 19 Aug 2009; published 26 Aug 2009

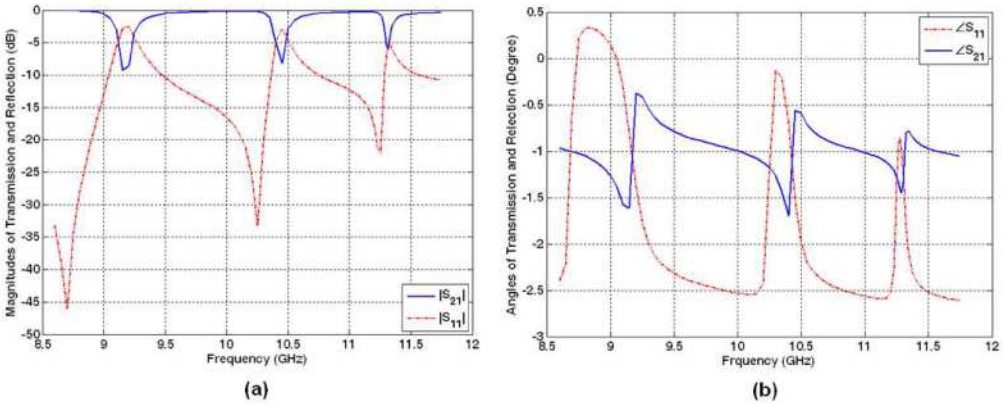

Fig. 14. Transmission and reflection characteristics for the composite cell shown in Fig. 13. (a) Magnitude in dB, (b) Phase in degree.

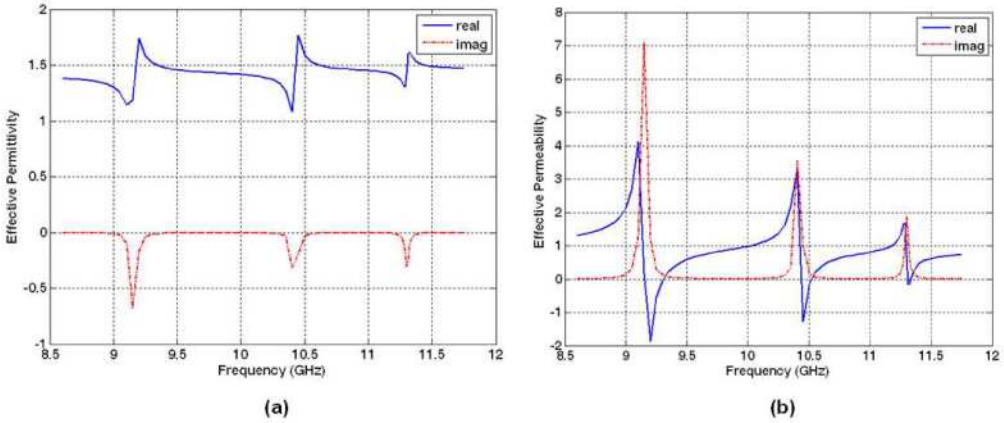

Fig. 15. Effective medium parameters for the composite cell shown in Fig. 13. (a) Effective permittivity, (b) Effective permeability.

#113866 - $15.00 USD Received 6 Jul 2009; revised 16 Aug 2009; accepted 19 Aug 2009; published 26 Aug 2009